Applied Physics Letters PERSPECTIVE scitation.org/journal/apl

Solution processed organic thermoelectric generators as energy harvesters for the Internet of Things

Cite as: Appl. Phys. Lett. **121**, 230501 (2022); doi: 10.1063/5.0129861
Submitted: 7 October 2022 · Accepted: 15 November 2022 ·
Published Online: 6 December 2022

Nathan Pataki,[1,2] Pietro Rossi,[1,2] and Mario Caironi[1,a)]

AFFILIATIONS

[1]Center for Nano Science and Technology @ PoliMi, Istituto Italiano di Tecnologia, Via Giovanni Pascoli, 70/3, Milano 20133, Italy
[2]Department of Physics, Politecnico di Milano, Piazza Leonardo da Vinci 32, Milano 20133, Italy

[a)]Author to whom correspondence should be addressed: mario.caironi@iit.it

ABSTRACT

Organic thermoelectric generators (TEGs) are a prospective class of versatile energy-harvesters that can enable the capture of low-grade heat and provide power to the growing number of microelectronic devices and sensors in the Internet of Things. The abundance, low-toxicity, and tunability of organic conducting materials along with the scalability of the fabrication techniques promise to culminate in a safe, low-cost, and adaptable device template for a wide range of applications. Despite recent breakthroughs, it is generally recognized that significant advances in *n*-type organic thermoelectric materials must be made before organic TEGs can make a real impact. Yet, in this perspective, we make the argument that to accelerate progress in the field of organic TEGs, future research should focus more effort into the design and fabrication of application-oriented devices, even though materials have considerable room for improvement. We provide an overview of the best solution-processable organic thermoelectric materials, design considerations, and fabrication techniques relevant for application-oriented TEGs, followed by our perspective on the insight that can be gained by pushing forward with device-level research despite suboptimal materials.

I. INTRODUCTION

The need for micro-power sources is rapidly growing as the web of connected sensors and devices known as the Internet of Things (IoT) begins to expand.[1] The possibility to collect and transmit valuable data has already led to applications in energy tracking,[2] security systems,[3] controllers,[4] transportation systems,[5] wearable electronics,[6] environmental monitoring,[7] and the use-cases will continue to grow.[8] The variety of connected sensors and devices means that there is a wide range of power demands spanning from 10 nW to 100 mW, but the demands of smaller nodes operating with efficient standby and communication, such as Bluetooth Low Energy (BLE), can range from just 100 nW to 10 mW.[9,10] Even for this smaller range of consumption characteristics, an assortment of affordable and low-maintenance energy harvesters is needed to accommodate the different environments, size-constraints, and price points.[11] Photovoltaics are part of the solution, but a complementary approach that can power microelectronics in dark conditions, such as in the dark server room or at night, is still needed.[1,12,13] Thermoelectric generators (TEGs) are proposed as the other half of the solution given their ability to generate electric current from otherwise wasted heat.[1,13] TEGs exploit the electromotive force resulting from entropy induced by thermodiffusion of free charge carriers in a material experiencing a thermal gradient, also known as the Seebeck effect.[14–16] When neither electrons nor holes prevail, the free charge carriers diffuse from the hot side of the material to the cold side and recombine.[17] In *p*- and *n*-type doped semiconductors, holes and electrons, respectively, are the majority charge carrier and dominate charge diffusion, resulting in an electrical potential between the hot and cold ends which can be exploited to power small electronic devices.[16,17] The Seebeck coefficient of a material is defined as the proportionality constant between the thermovoltage observed and the temperature gradient applied given as follows:[16]

$$S = -\frac{\Delta V}{\Delta T}. \tag{1}$$

Inorganic semiconductors and semimetals, such as Sb_2Te_3 and Bi_2Te_3, are used in high-performance TEGs, but these devices also

carry a high cost of materials, the need for energy-intensive processing, high toxicity to humans and their surroundings, and limited versatility with respect to applications.[16] Organic thermoelectric materials are generally seen as a complement to inorganic materials, not a like-for-like replacement, since inorganic TEGs will continue to be excellent power generators for purposes such as space exploration and high-temperature industrial applications. Organic thermoelectric materials, on the other hand, are ideal for harvesting low-grade heat (<200 °C) and supplying power to distributed applications with power consumption characteristics on the scale of 1–100 μW,[1] such as gas sensors,[18,19] transmitters,[20] image sensors,[21] and pressure sensors.[22] Many of the conjugated polymers and organic small molecules that are relevant for organic TEGs are derived from Earth-abundant elements and an increasing number can be synthesized using a "green" approach,[23] which offer safer, more affordable, and sustainable building blocks for low-power TEGs.[24,25] Organic semiconductors can also be synthesized to be solution-processable at ambient conditions, allowing deposition by large-area printing techniques making the design and fabrication of TEGs flexible and scalable. Additionally, organic semiconductors are highly tunable. Band structures, dopant miscibility, solubility, thermal conductivity, and more can be rationally altered with processing techniques, functionalization of the backbone, or modification of side chains.[15,26] Organic TEGs could be a cheap, non-hazardous, maintenance-free alternative power source for the billions of low-power sensors and electronic devices that make up the ever-expanding IoT.[1,12,13]

While the potential impact is high, examples in the literature of solution-processed organic TEGs are scarce, and those which can be found are rarely application-oriented or lack a viable *n*-type semiconductor.[27–30] Until now, the proof-of concept or unipolar, i.e., *p*-type only, TEGs of the past have been common, due to the limited performance and stability of *n*-type thermoelectric materials, but the library of *n*-type semiconductors and strategies to improve material properties have grown drastically. In this Perspective, we make an argument that future research should focus more effort into the design and fabrication of application-oriented TEGs using the organic thermoelectric materials currently at our disposal. In this context, an application-oriented TEG can be thought of as any device that aims to deliver an output power density >1 μW cm^{-2} (meaning that a TEG of 1–10 cm^2 could supply between 1 and 100 μW and a power output suitable for some low-power sensors[18,19,22] and electronics[20]) is sensibly designed to maximize efficient thermal coupling with a specific heat source and considers the stability of the device in the intended operating environment over an extended period of time. Even if a stable, scalable, and high-performing TEG is beyond reach with the organic thermoelectric materials currently at our disposal, by designing, fabricating, and testing organic TEGs that are more application-oriented, the community will build a valuable catalog of real-world designs, scalable fabrication methods, durable encapsulation techniques, innovative ways to integrate the devices into the environment, and pioneering approaches to couple TEGs with other energy harvesters which will be crucial for the rapid and efficient transfer of technology from the lab to the real-world. Section I of this Perspective aims to give the reader a brief overview of some constantly improving organic thermoelectric systems and property-enhancement strategies that could readily be employed in an application-oriented TEG. Section II provides the reader with some considerations relevant for designing and fabricating a solution-processed organic TEG. In Sec. IV, we make the case for more application-oriented TEGs, even if there is still considerable progress to be made on the thermoelectric materials themselves.

II. ORGANIC THERMOELECTRIC MATERIALS FOR TEGs

A prerequisite for any organic conducting or semiconducting material is a contiguous network of π-bonds between adjacent sp^2-hybridized atoms resulting in a π-conjugated structure.[31] The overlap between π-orbitals leads to the formation of molecular orbitals in which charge carriers may delocalize and move along a conjugated backbone, if energetics permit, resulting in charge carrier conduction.[17] Extrinsic doping of organic semiconductors is a common method to increase the charge carrier density, resulting in *p*-type and *n*-type doped semiconductors, where holes and electrons, respectively, are the majority charge carrier. As previously mentioned, the majority charge carrier of the semiconductor will dictate the sign of thermovoltage, but the material properties relevant for a thermoelectric device are not entirely described by the Seebeck coefficient. The performance is also dependent on the ability of the material to conduct electrical current and impede heat flow.[32,33] The competing nature of the Seebeck coefficient, electrical conductivity, and thermal conductivity is typically represented in dimensionless figure of merit, zT, which is used to gauge the thermoelectric performance

$$zT = \frac{\sigma S^2}{\kappa_e + \kappa_l} T, \tag{2}$$

where T is the temperature, σ is the electrical conductivity, κ_e is the charge carrier component of thermal conductivity, and κl is its lattice component. The ideal thermoelectric material would, therefore, have the properties of a phonon-glass and electron-crystal, exhibiting high electrical conductivity but low thermal conductivity.[33] Organic semiconductors excel as phonon-glasses, typically displaying very low overall thermal conductivities between 0.1 and 1.0 W m^{-1} K^{-1},[34] due to a high degree of structural disorder,[35] but they typically demonstrate poor electrical conductivities due to the same structural disorder.[14,15] For this reason, more effort has been devoted to improving the electrical conductivity, and the performance is reported simply using the power factor, $PF = \sigma S^2$.[14] Since the first studies on conducting and semiconducting organic materials in the late 1970s,[31,36,37] there have been steady improvements in PF and zT for both *p*- and *n*-type thermoelectric materials. There is still a great deal of room for improvement, particularly for *n*-type systems, but the selection of solution-processable organic thermoelectric materials below is some of the most suited for an application-oriented TEG.

A. *p*-type thermoelectric materials for TEGs

A large number of *p*-type organic semiconducting systems, including polyacetylenes, polyanilines, and polythiophenes have extensively been studied over the past decades;[14,15,25,38] however, no *p*-type material has had a bigger impact on the field of organic thermoelectrics than poly(3,4-ethylenedioxythiophene):poly(styrenesulfonic acid) (PEDOT:PSS).[39,40] In its *p*-doped state, the positively charged PEDOT chain is stabilized by the negative counterion, PSS, and through tunable secondary doping PEDOT:PSS can achieve electrical conductivities far beyond 1000 S cm^{-1}.[41–43] Along with excellent electrical conductivity, PEDOT:PSS is attractive as a thermoelectric material due to a non-negligible Seebeck coefficient, typically ranging

between 10 and 40 μV K^{-1},[43–45] mechanical flexibility, thermal and atmospheric stability, and solution-processability.[46] Commercial formulations of PEDOT:PSS inks tailored for ink-jet printing and screen printing have widely been accessible for years. The high performance, stability, accessibility, and versatility of PEDOT:PSS has made it one of the preferred choices for the *p*-type semiconductor in the reported hybrid and organic TEGs.[24,47,48]

In addition to PEDOT:PSS, other *p*-type materials, such as poly(3,4-ethylenedioxythiophene) doped with iron(III) p-toluenesulfonate (PEDOT:Tos),[49,50] poly(2,5-bis(3-dodecyl-2-thienyl)thieno[3,2-*b*]thiophene) (PBTTT),[51,52] and poly(3-hexylthiophene) (P3HT),[53] have been shown to have excellent thermoelectric properties. There are reports of PEDOT:Tos demonstrating $PF > 70\,\mu$W m^{-1} K^{-2},[49,50] and a highly aligned PBTTT film was shown to have an electrical conductivity of up to 2400 S cm^{-1} and $PF \approx 530\,\mu$W m^{-1} K^{-2}.[51] When it comes to choosing a *p*-type thermoelectric material for a TEG, there is no shortage of high-performing, stable materials,[14,15] but still the wide availability and versatility of PEDOT:PSS make it one of the very best choices.

B. *n*-type thermoelectric materials for TEGs

Achieving a stable, highly conductive *n*-doped organic semiconductor has considerably been more difficult than for *p*-type systems, although very recently Tang *et al.* have demonstrated a high performing *n*-type polymer, poly(benzodifurandione) (PBFDO), with $\sigma_{max} > 2000$ S cm^{-1} that could potentially close the gap between *zT* values of *n*- and *p*-type materials.[54] One of the challenges for *n*-type systems is the small number of available electron-withdrawing building blocks that also exhibit stable electron transport characteristics.[55] For stable transport in the doped state, the acceptor moiety in the organic semiconductor should have a sufficiently high electron affinity (EA), which translates to a low-lying energy level of the lowest unoccupied molecular orbital (LUMO), to avoid de-doping oxidation reactions in ambient air.[55] Theoretical calculations and empirical data show that to obtain a stable *n*-doped state, an organic semiconductor should ideally have a LUMO energy, E_{LUMO}, less than –4.0 eV.[56–59] A low E_{LUMO} would also energetically favor charge transfer from the highest occupied molecular orbital (HOMO) of the electron-donating dopant molecule or from the singly occupied molecular orbital (SOMO) in case a multi-step doping process.[60,61] In addition to the ionization potential of the dopant and the EA of the host, the molecular size and shape of *n*-type dopants and vicinity to the conjugated backbone will affect the doping efficiency, charge carrier concentration, and, thus, the electrical conductivity.[62]

1. n-type dopants for TEGs

When considering TEG fabrication, *n*-doping processes, such as mixed-solution doping (the dopant is dissolved in the same solution as the organic semiconductor before deposition) or sequential-solution doping (the dopant is dissolved in an orthogonal solvent with respect to the film and the film is soaked or coated in the dopant solution), are easier to implement than a method such as sequential-vapor doping (the dopant is volatilized in a closed chamber containing the cast film).[63] There are a number of different classes of soluble *n*-dopants including benzimidazoles,[64–67] amines,[68,69] carbenes,[70,71] and phosphines[69,72] which could be considered for TEGs. Some of the most widely studied and commercially available high performing *n*-type dopants include 1,3-dimethyl-2–2-phenyl-2,3-dihydro-1H-benzoimidazole (N-DMBI), (pentamethylcyclopentadienyl)(1,3,5-trimethylbenzene)ruthenium dimer [RuCp*Mes]$_2$,[73–75] and 1,5,7-triazabicyclo [4.4.0] dec-5-ene (TBD).[76,77] Other *n*-dopants, such as triaminomethane (TAM)[68,78] and 1,3-dimethylimidazolium-2-carboxylate (DMImC),[70,78] have a smaller molecular volume and improved miscibility with the host, but these are not commercially available at high purities. In general, *n*-type dopants tend to demonstrate low doping efficiencies, sometimes falling below 1%[64,79] which can be prohibitive for TEGs, but strategies like functionalization of the dopant or host to improve miscibility[80,81] and processing techniques[67,82,83] have been shown to improve the doping efficiencies. More recently, it has also been shown that transition-metal nanostructures on the substrate can act as catalysts for the single electron transfer of *n*-type dopants to acceptors, thus improving the doping efficiency of some systems by as much as 100-fold.[84]

2. n-type semiconductors for TEGs

Organic *n*-type semiconductors are often seen as the limiting factor for application-oriented solution-processed TEGs, because there is not a widely available material which exhibits high electrical conductivity, a reasonable negative thermovoltage, solution processability, and ambient stability, although there are claims that PBFDO could potentially be that breakthrough material.[54] Despite the fact there is no clearly superior *n*-type thermoelectric material, the concerted effort to find such a material has resulted in several examples of solution-processable *n*-type organic semiconductors which can, and should, be put to use in application-oriented TEGs. Some of the most reported *n*-type materials include diimide-based polymers, diketopyrrolopyrrole-based polymers (DPP), and fullerene derivatives.[15,55]

A napthalene diimide-based polymer, poly{N,N′-bis(2-octyl-dodecyl)-1,4,5,8-napthalenedicarboximide-2,6-diyl]-alt-5,5′-(2,2′-bithiophene)} (PNDI-T2), was initially reported in 2008,[85] and since then PNDI-T2 and other naphthalene diimide (NDI) derivatives have thoroughly been investigated.[56,65,86–91] A wide range of dopants, including 1-H-benzimidazole[64,67,92] amines,[91,93,94] anions,[95] radical cations,[96] and metallocenes,[97–99] have been used to *n*-dope PNDI-T2, but the electrical conductivity of the resulting films has not surpassed 10^{-2} S cm^{-1} which is very limiting for any meaningful use in a TEG. Despite that, different strategies have been used to improve the electrical conductivity, dopant-miscibility, film structure, and stability of PNDI-T2 and other NDI-based polymers, such as side chain engineering,[80,100,101] end group control,[90] and modification or substitution of the copolymer backbone.[65,86,91,102–105] A PNDI-T2 derivative with triethylene glycol side chains, PNDI2TEG-2Tz, synthesized by Liu *et al.*, remains one of the best performing NDI-based organic semiconductors, reaching a $\sigma_{max} = 1.8$ S cm^{-1} and $PF_{max} = 4.5\,\mu$W m^{-1} K^{-2} when doped with N-DMBI.[101] Despite considerable improvements to the electrical conductivity of doped NDI-based polymers, the stability of the doped state in air is still a challenge. Most PNDI-T2 derivatives have an E_{LUMO} between −3.69 and −3.76 eV,[88,101,104] meaning that the reduced state of the organic semiconductors is still susceptible to interaction with oxygen and water. De-doping occurs rapidly for thin films, and the electrical conductivity of these NDI polymers typically decreases by several orders of magnitude within an hour after taking a sample out of the glovebox.[104] Thionation of PNDI-T2 has been shown

to lower the E_{LUMO} to −3.96 eV, resulting in a relatively stable doped state over 16 h, but with a limited σ_{max} just above 10^{-3} S cm^{-1}.[104]

Lactam-lactone-based polymers, like benzodifurandione-based polyphenylenevinylene (BDPPV), are another class of promising *n*-type organic semiconductors for TEGs. Pei and co-workers have published several studies on BDPPV-based polymers doped with well-known *n*-type dopants including N-DMBI and TAM that have demonstrated outstanding thermoelectric properties with σ_{max} ranging from 14 to 90 S cm^{-1}.[68,73,106–109] In addition, BDPPV and its derivatives like ClBDPPV and FBDPPV have an E_{LUMO} below −4.0 eV due to carbonyl groups with strong electron-withdrawing characteristics,[107,110,111] although long-term stability testing in a TEG has yet to be confirmed.

Poly(benzimidazobenzophenanthroline) (BBL) is another good electron transporting, highly planar, semiconducting polymer that has recently gained attention after Yang *et al.* developed a stable *n*-type ink in combination with the amine-based *n*-dopant, polyethylenimine (PEI).[112] The films spray-coated from the ethanol-based BBL:PEI ink demonstrated σ_{max} up to 8 S cm^{-1} and a $PF_{max} = 11\ \mu$W m^{-1} K^{-2}.[112] The BBL:PEI ink was also shown to be air-stable over the course of 24 h, which is promising for TEG applications, although the method of deposition seems to be limited to spray-coating for now.[112]

Small molecule fullerene derivatives, such as [6,6]-phenyl-C_{61}-butyric acid methyl ester (PCBM), have extensively been studied for organic photovoltaic applications,[113,114] but modifications of fulleropyrrolidine with oligoethylene glycol (OEG) side chains have demonstrated record high *zT* values, above 0.3, for *n*-type organic thermoelectric materials.[115] The excellent thermoelectric performance of the fullerene derivative, PTEG-2, is due in part to the ethylene glycol side chains, which have been shown to improve dopant miscibility resulting in $\sigma_{max} > 10$ S cm^{-1}.[115] The other huge advantage of the fullerene derivatives synthesized by Koster and co-workers (PTEG-2, PTEG-1, PDEG-1, PPEG-1, etc.) are their exceptional Seebeck coefficients, in the framework of doped organic materials, ranging from ∼−200 μV K^{-1} when overdoped to an outstanding ∼−600 μV K^{-1} at low doping concentrations.[81,116,117] The PF_{max} of PTEG-2 surpasses 40 μW m^{-1} K^{-2} making it one of the best *n*-type candidates for a TEG.[115]

The dopants and semiconductors listed above are those which we believe to have the highest potential to be incorporated into an application-oriented TEG, but they make up a small subsection of organic thermoelectric materials as a whole. There are several comprehensive reviews giving a more complete account of organic thermoelectrics.[14,15,25,78] Furthermore, the section above primarily focuses on electrical conductivity as the distinguishing property between materials, but the sections below will present a number of different strategies to influence thermal conductivity, thermovoltage, and morphology of a thermoelectric material that can be employed to enhance the overall performance of a TEG.

C. Suppression of thermal conductivity

Typically the thermal conductivities of polymers and small molecules are advantageously low, but achieving control over and additionally suppressing thermal transport properties of organic semiconductors could be an useful approach to improve their thermoelectric performance.[34,118] In most organic thermoelectric materials, the electronic contribution to thermal conductivity is much lower than the lattice or phonon component, $\kappa_e \ll \kappa_l$ and is often considered negligible with respect to *zT* [Eq. (2)].[34,119,120] The lattice contribution is also greatly suppressed due to structural disorder of most organic semiconductors, resulting in low overall thermal conductivities typically ranging from 0.1 to 1.0 W m^{-1} K^{-1}.[34,65] Phonons in these disordered systems are localized, and the localized lattice vibrations can be described by the Einstein model of isolated atomic oscillations that transfer heat through a random walk mode rather than through collective lattice oscillations.[121,122] Selezneva and co-workers took advantage of this fact to further localize the lattice vibrations of dinaphtho[2,3-b:2′,3′-f]thieno[3,2-b]thiophene (DNTT) by adding long terminal alkyl chains to the molecular semiconductor (C8-DNTT-C8).[122] The addition of the long alkyl terminal chains was found to reduce of the spatial extension of the vibrational modes and thereby reduced the in-plane thermal conductivity of C8-DNTT-C8 to an exceptionally low 0.05 W m^{-1} K^{-1}.[122]

Zapata-Arteaga *et al.* also successfully demonstrated the suppression of the lattice component of thermal conductivity by tuning the annealing temperature of poly(2,5-bis(3-alkylthiophen-2-yl)thieno[3,2-b]thiophene) (PBTTT) to induce a more crystalline microstructure, followed by low doping concentrations (<1 mol. %) of 2,3,5,6-tetrafluoro-7,7,8,8-tetracyanoquinodimethane (F4TCNQ).[123] The annealing results in larger polymeric crystalline domains and increases the thermal conductivity as thermal percolation is established, after which the small amount of F4TCNQ causes an effect similar to alloy-scattering seen in inorganic materials and reverses the increase in thermal conductivity by a factor of two without affecting the crystallinity.[123] Although slightly more niche, strategies like these could be used in the right circumstances to improve the overall *zT* of a thermoelectric material and improve the performance of a TEG.

D. Enhancing the Seebeck coefficient

The most basic model for homogeneous materials relates the Seebeck coefficient directly to the conductivity of the density of states (DOS), σ(E),[14]

$$S = -\frac{k_B}{e}\int \frac{E - E_F}{k_B T}\frac{\sigma(E)}{\sigma}dE, \tag{3}$$

where k_B is the Boltzmann constant, *e* is the elementary charge, E_F is the Fermi level, *T* is the temperature, and σ is the electrical conductivity. Doped organic semiconductors typically have charge carrier concentrations that exceed the Boltzmann limit, and Eq. (3) can be simplified to $S = (E_F - E_{tr})/T$, where charge transport in organic semiconductors occurs between the Fermi energy and transport energy.[124,125] The Fermi level of the doped organic semiconductor will edge closer to the transport level as charge carrier concentration increases due to doping, and the transport level, which is near the maximum of a Gaussian DOS,[14] does not move unless the DOS changes.[17] The result of increasing charge carrier concentration through doping is a decrease in Seebeck coefficient, which has been shown to hold true over a broad range of doped organic materials. An empirical relationship between the Seebeck coefficient and the electrical conductivity is found, $S \propto \sigma^{-1/4}$.[14] Tuning the charge carrier concentration in a single phase forces a trade-off between electrical conductivity and thermopower in order to maximize the *PF*, but a sensible design of DOSs in hybrid materials offers a promising strategy to

partially decouple the Seebeck coefficient from the electrical conductivity, potentially leading to further improved *PF*s.[126] Zuo *et al.* have demonstrated that it is possible to mix materials with significantly different HOMO levels to split the Fermi level and transport level across the two peaks of the doubly peaked DOS for the hybrid material to obtain record-breaking Seebeck coefficients for electronic thermoelectrics, ~2000 μV K^{-1}.[126] To date, this hybrid-system strategy has not yet produced a *PF* that outperforms the single system, but trying to push thermovoltage of an organic thermoelectric material to its limits could be a fresh alternative to improving materials for TEGs, if compatible architecture and processes are devised.

E. Control of morphology

As for any other organic electronic device, structure–property relationship in organic solids is a key for optimizing TEGs. Understanding and controlling the morphology of thin film organic semiconductors during the TEG fabrication process is a powerful tool to boost the thermoelectric performance of the device. After a thermoelectric ink is deposited, the microstructure of the semiconducting film can range from highly disordered and amorphous-like to semicrystalline and because the charge carrier transport is dominated by interchain coupling, the morphology of the film can have a large impact on *zT*.[15] In addition to interchain proximity, the conformation of a single conjugated backbone, including defects like twisted and kinked chains, will affect the species' intrachain charge carrier mobility.[15,17] It would follow that thermoelectric films with less defects and higher degrees of crystallinity will have superior properties, and this is true in some cases,[103,127] but the relationship is not so simple across all systems.

Highly ordered PEDOT, poly(3-hexylthiophene-2,5-diyl) (P3HT) and polyaniline have demonstrated improvements in both electrical conductivity and *p*-type Seebeck coefficient when methods, such as changing the polarity of the solvent,[119] exploiting a crystalline template during epitaxial growth,[53] or adding self-assembled supramolecules,[128] were used to influence a more ordered film morphology. Morphological changes can also be induced post-deposition with methods such as the high-temperature rubbing technique first reported for highly conductive organic thermoelectric materials by Brinkmann[129] and later investigated by Sirringhaus and colleagues.[130] An intriguing aspect of polymer chain alignment is to increase conductivity by enhancing charge-carrier mobility without modifying charge density, thus, not sacrificing the Seebeck coefficient. In this respect, a high-temperature rubbing technique was recently shown to uniaxially align the polymer chains of poly(2,5-bis(3-dodecyl-2-thienyl)thieno[3,2-b]thiophene) (PBTTT) resulting in a σ_{max} of up to 4345 S cm^{-1} for transport parallel to the polymer chains, a conductivity four times greater than that of the unaligned films, while the Seebeck coefficient remained nearly unchanged.[130]

Rational design of the polymers has been another approach to influence backbone orientation and thermoelectric performance. *n*-type copolymers with naphthodithiophenediimide (NDTI) and bithiopheneimide (BTI) units were polymerized to investigate the impact of a bimodal orientation on electrical conductivity.[131] It was found that the copolymer with bimodal orientation, both face-on and edge-on orientations, led to the formation of 3D conduction channels and the better accommodation of dopants, resulting in a σ_{max} of 11.6 S cm^{-1} and *PF* of 53.4 μW m^{-1} K^{-2}.[131]

Again, the implications of microstructure in one system cannot always be applied to a different system. For example, unreacted or degraded dopant molecules can be viewed as defect and have deleterious effects in some systems,[62] while in other cases it can improve performance.[67] As N-DMBI is exposed to oxygen and moisture, the degradation by-product, DMBI-Ox, is formed and can no longer undergo the C–H bond cleavage needed for charge transfer to an *n*-type organic semiconductor.[82] DMBI-Ox can be seen as an impurity in some systems, but recent findings from Pallini *et al.* show that small amounts of DMBI-Ox can trigger the nucleation of small DMBI-H crystallites within PNDI-T2 and sizably improve the electrical conductivity, particularly at low doping levels.[67] The nuances of solid-state microstructure in organic semiconductors are complex, but there are huge improvements to be gained for a TEG if one can understand and influence the morphology of the thermocouples. That being said, the morphology of a film and the impact it might have on charge transport is highly specific to each semiconductor:dopant blend system and generalizations about crystallinity, alignment, phase segregation, and orientation should be used cautiously considering the current level of understanding. Transferring the gained knowledge regarding processing-structure–property relationships to TEGs will be a critical component in realizing high-performing devices, as TEG architectures and fabrication methods may pose constraints on the accessible processes.

III. DESIGN AND FABRICATION OF TEGs

Section III has outlined a range of organic thermoelectric materials and strategies to enhance their properties, yet their adoption in efficient TEGs is still quite limited and yet to be fully exploited. This section covers some of the design and fabrication considerations needed to turn a promising organic thermoelectric system into a functional TEG.

A. Stable ink formulation

Solution-processibility of organic semiconductors is undoubtedly one of the greatest advantages of organic thermoelectrics over inorganics, but developing an ink from a promising organic semiconductor that is stable and suitable for large-area deposition techniques requires many considerations depending on the material, solvent, and deposition method. Solubility, or at least the ability to be dispersed, of the polymer or small molecule is imperative if the ink's properties are to remain constant during the entire deposition process.[132,133] Ideally, once the active material is dissolved in the solvent, it will remain in solution, with no sign of precipitation or agglomerate formation, for an indefinite amount of time. A few common solvents for organic semiconductors and small molecule dopants include *ortho*-dichlorobenzene (*o*-DCB), chlorobenzene (CB), toluene, and *ortho*-xylene. However, there is a strong push to develop inks that make use of "green" or non-hazardous solvents, such as water, ethanol, butanol, or isopropanol.[132] Long-term stability of the formulations in these green solvents might not always be possible, but dispersants, surfactants, and solvent-exchange methods can be used to achieve dispersions suitable for uniform deposition.[132,133] BBL is an example of an organic polymer that is only fully soluble in strong protonic acids such as methanesulfonic acid (MSA),[134] but it was demonstrated that a solvent exchange from MSA to ethanol can be used to obtain a green BBL-based ink.[112] Commercial formulations of PEDOT:PSS, gold,

and silver nanoparticles are other examples that employ methods of assisted solubility to achieve high-performing inks in non-hazardous solvents like water.[135]

Properties, such as viscosity, surface tension, and volatility, must also be considered for a stable ink formulation and should be adjusted depending on the desired deposition technique. For example, with ink-jet printing, the fluid properties of the ink will dictate the acoustic dampening of the pressure waves applied by the piezoelectric actuator, thereby influencing the jet stability and droplet volume and velocity.[136] On the other hand, methods like screen or gravure printing will require entirely different rheological properties, and one might have to tune the viscosity or surface tension with binders, surfactants, or binary mixtures of solvents.[133,137] Solvent volatility is also a key attribute of the ink formulation, and an ink with a low boiling point (BP) could be ideal for a deposition method like spray-coating where aerosolized droplets should dry quickly after deposition before another coat can be applied. On the other hand, ink-jet printing requires less volatile solvents (BP $> 90\,^{\circ}$C) for proper droplet formation.

B. Design and fabrication

The core architecture of any TEG is remarkably simple: alternating *p*- and *n*- type legs connected electrically in series and thermally in parallel [Fig. 1(a)]. However, when one considers the vast variety of temperature gradients and the numerous fabrication techniques that can be exploited, the diversity of organic TEG architectures becomes apparent. For example, the radial thermal gradient between a human wrist and the air is quite different from the vertical temperature difference between the surface of the ocean and water 3 m below the surface; therefore, the optimized TEGs for each use-case would look very different. Even if two heat sources appear to have similar directionality, e.g., a human wrist and a car exhaust pipe both with radial heat fluxes between the interface with air, the magnitude of the temperature difference, the radius of curvature, and thermal contact resistance would lead to two entirely different TEG designs. This is radically different from organic solar cells, for example, where the reference source, i.e., the radiation spectrum impinging on the device, is well described by standards depending on the geolocalization.[138] In this case it is much more obvious to have a common reference high-level architecture,

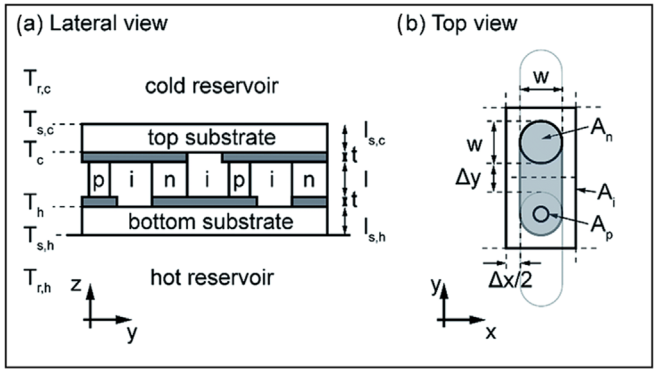

FIG. 1. (a) Cross sectional lateral sketch of a typical TEG architecture. (b) Top view sketch of a typical TEG architecture. Reproduced with permission from Beretta *et al.*, Sustainable Energy Fuels **1**, 174 (2017). Copyright 2017 The Royal Society of Chemistry.

which is not drastically changing, even when moving to artificial light conversion, e.g., for indoor applications.[139] The diversity in the thermal energy sources has profound implications for the development of TEGs with respect to other more main stream energy conversion devices, which will be further discussed in Sec. IV.

Rationally designing a TEG with an application in mind will require specific knowledge of the operating characteristics (voltage, power consumption during wake and sleep intervals, etc.) of the sensor or device, as well as a detailed understanding of the thermal gradient (geometry, thermal coupling characteristics, magnitude, and variability of temperatures, etc.).[140] The expected open circuit voltage of a TEG is given as $\boldsymbol{V_{TEG} = n(S_p - S_n)(T_H - T_C)}$, while the power output of the TEG is proportional to the fraction of the TEG footprint which is active material compared to the total footprint area, also known as fill fraction.[140] The fill fraction is defined as $\mathrm{FF} = A_{pn}/A_{pni}$, where $A_{pni} = A_p + A_n + A_i$ and $A_{pn} = A_p + A_n$, where the areas occupied by the *p*-type and *n*-type legs are A_p and A_n, respectively, and A_i is the area occupied by the insulator (Fig. 1).[140] Using the fill fraction, the power per unit area of a TEG is given as[140]

$$P_{\mathrm{density}} = \frac{\mathrm{FF}(S_p - S_n)^2}{\rho_{pn} l} \frac{m}{(1+m)^2} (T_h - T_c)^2, \tag{4}$$

where S_p and S_n are the Seebeck coefficients of the *p*- and *n*-type thermoelements, respectively, ρ_{pn} represents the weighted average electrical resistivity of one thermocouple such that $\rho_{pn} = (\rho_p/A_p + \rho_n/A_n)A_{pn}$, l is the length of the thermocouple, T_h and T_c are the temperatures of the hot and cold side of the TEG, respectively, m is the load resistance ratio where $m = R_{load}/nR_{pn}$ given that R_{load} is the load resistance, n is the number of thermocouples and R_{pn} is the resistance of one thermocouple. It can be seen that power output is largest under load-matching conditions, $m = 1$; therefore, designing a TEG such that the device resistance is close or equal to the resistance of the intended load can maximize the power output. Furthermore, the power output can be optimized with respect to the ratio between *p*- and *n*-type thermoelements[140]

$$\frac{A_p}{A_n} = \sqrt{\frac{\kappa_n \rho_p}{\kappa_p \rho_n}}, \tag{5}$$

where κ_n and κ_p are the thermal conductivities of the *p*- and *n*-type thermoelectric materials. It should be noted that power output optimized with Eqs. (4) and (5) are derived from a linearized model of energy conversion where Joule and Peltier effects are neglected.[140] The linearized model is suitable for a first iteration of an application-oriented TEG, but true optimization of the design with respect to the load and thermal gradient should consider the Joule and Peltier effects from circulating current in the TEG.[140] For further reading, Beretta *et al.* have derived a TEG's optimization conditions for both the non-linear and linear energy conversion models.[140] For an even more thorough simulation of the TEG's performance and thermal coupling to the environment, one should consider conducting finite element analysis.

Subsections III B 1–B 3 outline some common TEG architectures, fabrication methods, and examples of TEGs published in the literature.

1. Vertical architectures and fabrication methods

TEGs with a vertical architecture are those in which the thermocouples are perpendicular, or out-of-plane, with respect to the

substrate [Fig. 1(a)]. The prototypical inorganic or hybrid TEG has a vertical architecture where bulk materials are sintered to form rigid stand-alone columns sandwiched between two substrates that interface with the heat source and heat sink, but this architecture is less common among organic TEGs.[16] Vertical fabrication of a TEG using an organic thermoelectric ink has been achieved using substrate-assisted deposition, meaning that a precast substrate or mold will present wells to contain the ink while it is deposited.[141] A recent example of an organic perpendicular TEG from Massetti *et al.* was realized using femtosecond laser writing to embed conical micro-cavities directly in a polyethylene naphthalate (PEN) substrate, thus reducing inevitable thermal losses across the thickness of the substrate.[30] Several micro-cavities were used to defined each leg, which were then filled with PEDOT:PSS (*p*-type) and PTEG-1 (*n*-type) inks using a precision ink-jet deposition method (Fig. 2).[30] The vertical organic micro-TEG was able to deliver 30 nW cm^{-2} at $\Delta T = 25$ K.[30]

Fused deposition modeling (FDM), a common form of 3D-printing, has also been exploited to fabricate vertical TEGs.[141] FDM extrudes thermoplastic filaments through a heated nozzle resulting in out-of-plane deposition.[141] At the time of writing, very few examples of organic FDM filaments exist, but a PEDOT:PSS-polyethylene oxide composite[142] and a polyurethane/multi-walled CNT composite have recently been reported.[143] Most studied FDM filaments for TEGs are composites containing an inorganic active material and the polymeric component is simply limited to a thermoplastic binder.[144] Kee *et al.* demonstrated that a 3D-printed organic TEG could be achieved using a thermoelectric composite comprising of dimethyl sulfoxide (DMSO), PEDOT:PSS along with a polymeric surfactant as soft matrix.[145] The composite was in particular, formulated to exhibit self-healing properties and stretchability, and it retained >85% of its initial power output after repetitive cutting and 35% strain.[145] Although this particular 3D-printed TEG has a planar architecture, the PEDOT:PSS filament could also be used for vertical architectures.[145]

2. Planar architectures and fabrication methods

TEGs with a planar architecture are those in which the thermocouples and the substrate lie in the same plane. Organic thermoelectric inks are well suited for planar designs, due to the various printing techniques like ink-jet, screen, and gravure printing which can easily pattern such architectures. Planar architectures may also be patterned with standard techniques, such as lithography or chemical vapor deposition, but printing techniques that exploit thermoelectric inks are fast, affordable, and waste-reducing alternatives. Depending on the configuration, planar TEGs can intercept both in-plane and out-of-plane thermal gradients. For example, the origami-inspired folding process reported by Rösch *et al.*,[143] not only enabled the screen-printed planar TEG to intercept an out-of-plane thermal gradient, the conformational change also greatly increased the number of thermocouples per unit area and, thus, the power density [Fig. 3(a)]. An outstanding power

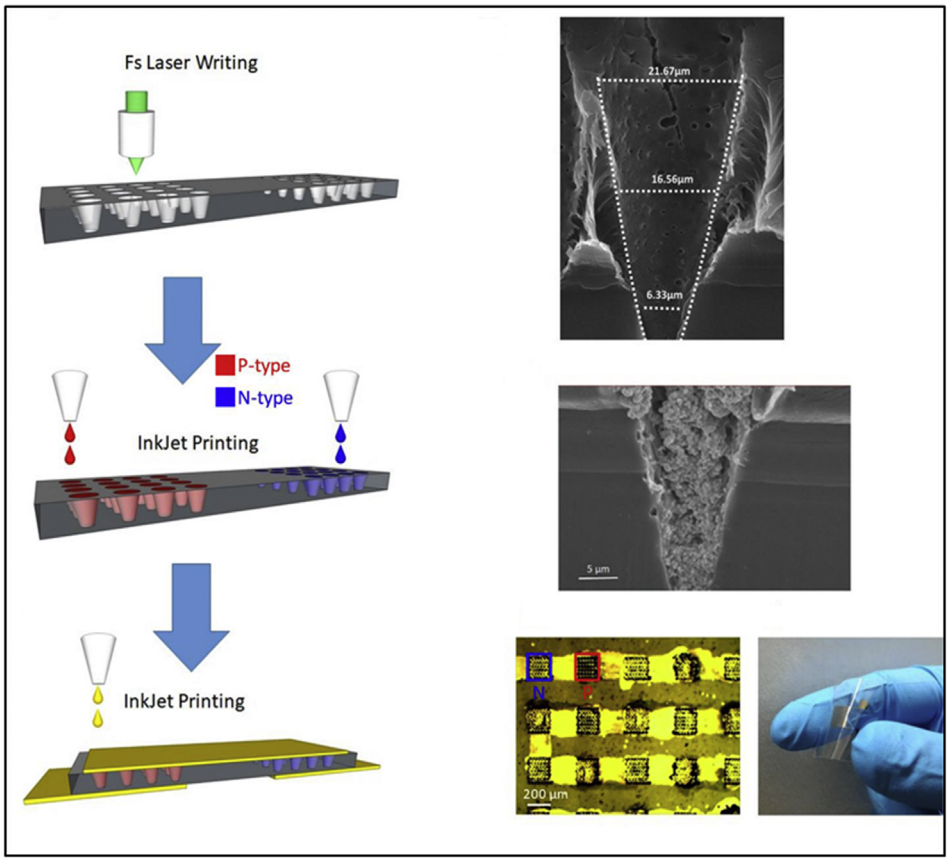

FIG. 2. Vertical organic micro-thermoelectric generator, using only direct writing methods, embedding the thermoelectric legs within a plastic substrate through a combination of direct laser writing and inkjet printing techniques. Reproduced with permission from Massetti *et al.*, Nano Energy **75**, 104983 (2020). Copyright 2020 Elsevier Ltd.

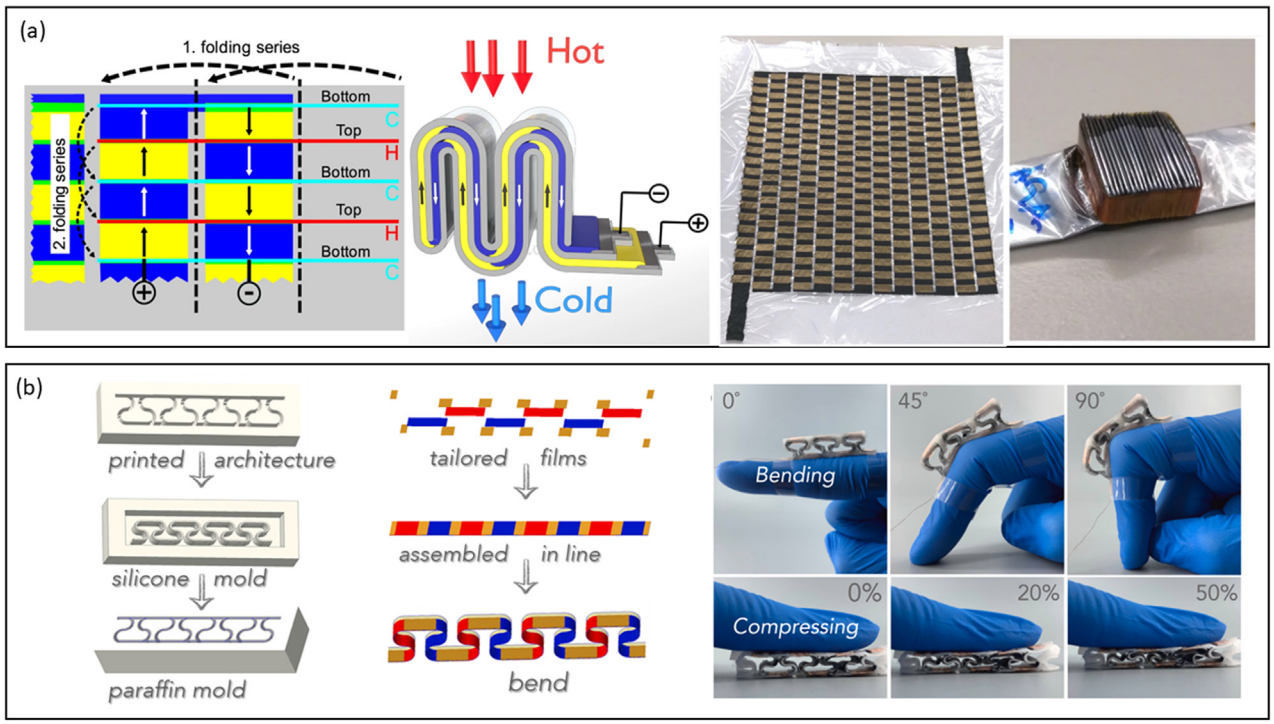

FIG. 3. (a) Origami-inspired folded design for a hybrid (organic/inorganic) thermoelectric generator, demonstrating one way in which a planar architecture can be conformed to intercept a vertical temperature gradient and increase thermocouple density. Reproduced with permission from Rösch *et al.*, npj Flexible Electron. **5**(1), 1–8 (2021). Copyright 2021 Authors licensed under a Creative Commons Attribution (CC BY) license. (b) A spring-shaped thermoelectric generator where carbon nanotube-based active materials are initially deposited as a thin film, then the planar architecture is transformed into a vertical device with the use of a paraffin mold. Reproduced with permission from Lv *et al.*, Nano Energy **88**, 106260 (2021). Copyright 2021 Elsevier Ltd.

density of 47.8 μW cm^{-2} at $\Delta T = 30$ K was reported for their origami TEG, although it should be mentioned that it was a hybrid device using PEDOT:PSS nanowires for the *p*-type legs and TiS_2:hexylamine-complex for the *n*-type legs.[143] Another creative example of conformational change is seen when a printed pattern is first folded, then inserted into a mold and filled with PDMS to achieve a flexible spring-shaped vertical TEG [Fig. 3(b)].[146] This spring-shaped TEG delivered a power output of ~749 nW, equal to a power density of ~416 nW cm^{-2}, at $\Delta T = 30$ K; yet, it should be noted that the thermoelectric materials in this case were carbon nanotubes (CNTs).[146]

3. Thermoelectric fibers

Many exciting potential applications for flexible organic TEGs revolve around wearable electronics. For wearable applications, it makes sense to aim for thermoelectric fibers that could be comfortably incorporated into a piece of clothing or accessory. Current strategies for achieving thermoelectric fibers include coating an existing fiber with active material or spinning a stand-alone fiber from the active materials. The first option can be problematic if the active material does not adhere well to the substrate fiber or if the charge percolation pathways degrade with time and use.[147] Cotton and cellulose have been used as a host for active materials with mixed results.[147–149] Cataldi *et al.* have shown that similar fiber-based TEGs can be realized by spray-coating cotton fibers with a mixture of doped nanocarbon species (active material) and aleuritic acid (binder) to produce a biodegradable composite for thermoelectric applications.[147] The proof-of-concept TEG made entirely from the organic textile-based thermocouples yielded a maximum power output of ≈1.0 nW at $\Delta T = 70$ K.[147] Spray-coated or solution-soaked thermoelectric fibers also have the benefit of being extremely scalable.

On the other hand, stand-alone spun fibers demonstrate better uniformity and thermoelectric performance, at the cost of simplicity and scalability.[150] In one example, a ternary flexible composite fiber based on the PEDOT:PSS, tellurium nanowires (Te-NWs), and polyvinyl alcohol (PVA) was used to make a TEG demonstrating an output voltage of 5.03 mV and power density of 28.87 μW cm^{-2} at $\Delta T = 60$ K.[151] It was also demonstrated that robust conducting polymer fibers could be made by wet-spinning of PEDOT:PSS into sulfuric acid, resulting in fiber-based TEG with an open circuit voltage of 7.9 mV and output power of 2.8 nW at $\Delta T = 40$ K (Fig. 4).[152] Thermoelectric fibers made by twisting floating catalyst synthesized CNT films can be sequentially doped to achieve a woven TEG with a peak power density of 70 mW m^{-2}.[153] Ding *et al.* utilized an even more complex colloidal gelation extrusion process to splice *p*- and *n*-type CNT segments together into a contiguous fiber.[150] The resulting fibers are both strong and flexible, and a woven fabric produced a power output of more than 80 μW at $\Delta T = 20$ K.[150]

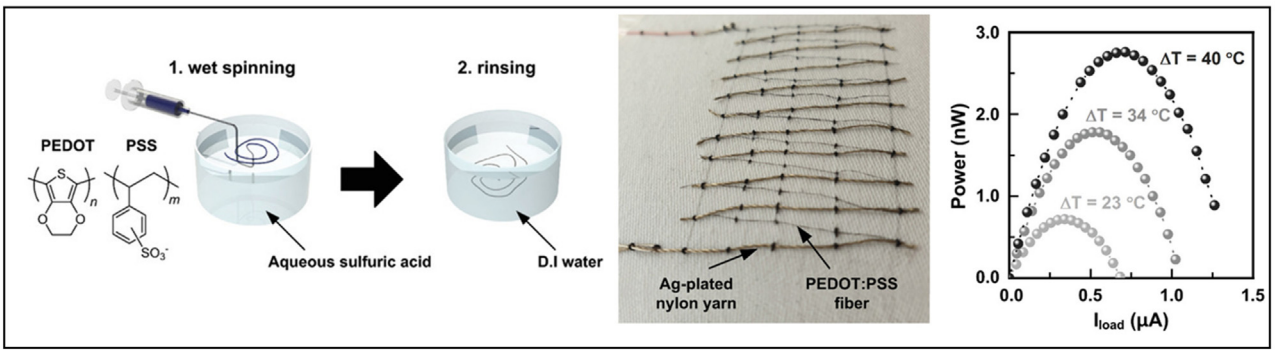

FIG. 4. Process of wet-spinning PEDOT:PSS fibers from sulfuric acid coagulation bath, the resulting fiber-based TEG and the power output of the TEG. Reproduced with permission from Kim *et al.*, Macromol. Mater. Eng. **305**(3), 1900749 (2020). Copyright 2020 Authors, licensed under a Creative Commons Attribution (CC BY) license.

IV. OUTLOOK

The sections above are meant to summarize the knowledge and expertise surrounding organic thermoelectric materials, device design, and fabrication techniques that have been achieved by the community as a whole and to provide a manageable, albeit optimistic, approach to creating an application-oriented organic TEG. The goal was not to downplay the shortcomings of organic thermoelectric materials, especially *n*-type ones, since it is clear that materials development will play a crucial role in allowing more efficient organic TEGs. Instead, the main motivation is to encourage more researchers to envision and execute specific TEG designs which more closely resemble the devices that will make a meaningful impact on powering the billions of microelectronic devices in the IoT. Unlike solar energy conversion, thermal energy conversion is relevant only for harvesting[154] and lacks a generalized and standard source. The thermal gradients arising from different potential application cases vary drastically in spatial distribution, average and boundary temperatures. This range of sources is immediately evident when comparing potential sources of waste heat like human body, a hot water pipe, soil or water. By focusing more attention on application-oriented TEGs, the community will build a valuable catalog of real-world designs, scalable fabrication methods, durable encapsulation techniques, innovative ways to integrate the devices into the environment, pioneering approaches to couple TEGs with other energy harvesters, and much more. When the materials breakthrough that can unlock a high-performing, stable and scalable organic TEG does occur, this catalog of application-oriented knowledge will be crucial for the rapid and efficient transfer of technology from the lab to the real-world.

To better illustrate the argument, it is interesting to consider the closely related field of organic photovoltaics (OPVs). Photovoltaic properties of organic materials like anthracene were being studied as early as the 1950s, but few or very simplistic photovoltaic cells were being made around this time.[155] By the 1970s, dyes like chlorophyll–*a* (Chl–*a*) were found to have a higher photocurrent quantum yield than its predecessors, but the real breakthroughs in power conversion efficiencies (PCE) of OPVs came from the discovery of bulk heterojunctions, which was a direct result of fabricating full photovoltaic cells with the materials on hand.[155,156] During this period, it became common for researchers working on OPVs to fabricate small 0.1 cm^2 cells as a way to compare OPV performance more uniformly. It was through the process of fabricating these fully functional, albeit small, photovoltaic cells that some of the largest improvements in PCE stemmed from exploring different electrode materials, heterojunctions and double layers, fabrication and encapsulation methods and more.[155] Since the discovery of bulk heterojunctions, OPV research has largely been materials driven with the goal of developing semiconductors with higher photocurrent quantum yield, but the breakthrough stemming from photovoltaic cell fabrication was critical to progressing the field and keep quantitative track of such progress. The field of organic thermoelectrics is now at a point where a similar enthusiasm for device design and fabrication is needed.

In fact, it could be argued that the vast diversity of use-cases (size and shape of the temperature gradient, biocompatibility, environmental stability, etc.) for organic TEGs means that tackling these design and engineering challenges is more pertinent for organic TEGs than for OPVs with a unidirectional power source, the Sun. The architectures, fabrication methods, encapsulation methods, environmental coupling, power outputs, and price-points will need to be optimized for every intended thermal gradient and application. Perhaps the vast range of potential use-cases and the unique optimization required for each scenario sounds like a Sisyphean task, but the large variety of applications is also what makes organic TEGs such an incredibly valuable energy source for the future.

ACKNOWLEDGMENTS

This work was supported by the European Union's Horizon 2020 research and innovation programme under the Marie Skłodowska–Curie Grant Agreement No. 955837.

AUTHOR DECLARATIONS

Conflict of Interest

The authors have no conflicts to disclose.

Author Contributions

Nathan James Pataki: Writing – original draft (lead); Writing – review & editing (equal); Conceptualization (equal). **Pietro Rossi:** Writing – review & editing (equal); Conceptualization (equal). **Mario Caironi:** Conceptualization (lead); Supervision (lead); Writing – review & editing (lead).

DATA AVAILABILITY

Data sharing is not applicable to this article as no new data were created or analyzed in this study.

REFERENCES

[1]M. Haras and T. Skotnicki, Nano Energy **54**, 461 (2018).
[2]K. Chooruang and K. Meekul, in International Conference on ICT and Knowledge Engineering, 2019, Vol. 48.
[3]S. Sruthy and S. N. George, in IEEE International Conference on Signal Processing, Informatics, Communication and Energy Systems (SPICES 2017), 2017.
[4]M. Bardwell, J. Wong, S. Zhang, and P. Musilek, in *Proceedings—IEEE World Congress Services (SERVICES)* (IEEE, 2018), p. 61.
[5]M. M. Rathore, A. Ahmad, A. Paul, and U. K. Thikshaja, in *Proceedings—IEEE Region 10 Symposium (TENSYMP 2016)* (IEEE, 2016), p. 135.
[6]W. Zeng, L. Shu, Q. Li, S. Chen, F. Wang, X.-M. Tao, W. Zeng, L. Shu, Q. Li, S. Chen, F. Wang, and X.-M. Tao, Adv. Mater. **26**, 5310 (2014).
[7]G. Mois, S. Folea, and T. Sanislav, IEEE Trans. Instrum. Meas. **66**, 2056 (2017).
[8]M. H. Miraz, M. Ali, P. S. Excell, and R. Picking, Future Internet **10**, 68 (2018).
[9]R. Schrader, T. Ax, C. Röhrig, and C. Fühner, in *IEEE 3rd International Symposium on Wireless Systems within the IEEE International Conferences on Intelligent Data Acquisition and Advanced Computing Systems (IDAACS-SWS 2016)—Proceedings* (IEEE, 2016), p. 62.
[10]K. Nair, J. Kulkarni, M. Warde, Z. Dave, V. Rawalgaonkar, G. Gore, and J. Joshi, in *Proceedings of the International Conference on Green Computing and Internet of Things (ICGCIoT 2016)* (IEEE, 2016), p. 589.
[11]M. K. Mishu, M. Rokonuzzaman, J. Pasupuleti, M. Shakeri, K. S. Rahman, F. A. Hamid, S. K. Tiong, and N. Amin, Electronics **9**, 1345 (2020).
[12]H. Elahi, K. Munir, M. Eugeni, S. Atek, and P. Gaudenzi, Energies **13**, 5528 (2020).
[13]S Zeadally, F. K Shaikh, A Talpur, and Q. Z Sheng, Renewable Sustainable Energy Rev. **128**, 109901 (2020).
[14]B. Russ, A. Glaudell, J. J. Urban, M. L. Chabinyc, and R. A. Segalman, Nat. Rev. Mater. **1**, 16050 (2016).
[15]M. Massetti, F. Jiao, A. J. Ferguson, D. Zhao, K. Wijeratne, A. Würger, J. L. Blackburn, X. Crispin, and S. Fabiano, Chem. Rev. **121**, 12465 (2021).
[16]D. Beretta, N. Neophytou, J. M. Hodges, M. G. Kanatzidis, D. Narducci, M. Martin-Gonzalez, M. Beekman, B. Balke, G. Cerretti, W. Tremel, A. Zevalkink, A. I. Hofmann, C. Müller, B. Dörling, M. Campoy-Quiles, and M. Caironi, Mater. Sci. Eng., R **138**, 100501 (2019).
[17]D. Scheunemann, E. Järsvall, J. Liu, D. Beretta, S. Fabiano, M. Caironi, M. Kemerink, and C. Müller, Chem. Phys. Rev. **3**, 021309 (2022).
[18]L. C. Tien, H. T. Wang, B. S. Kang, F. Ren, P. W. Sadik, D. P. Norton, S. J. Pearton, and J. Lin, Electrochem. Solid-State Lett. **8**, G230 (2005).
[19]L. Fan, N. Xu, H. Chen, J. Zhou, and S Deng, Sens Actuators, B **346**, 130545 (2021).
[20]T. K. Tsang and M. N. El-Gamal, in Proceedings—IEEE International Symposium on Circuits and Systems 2006, Vol. 670.
[21]S. Hanson, Z. Foo, D. Blaauw, and D. Sylvester, IEEE J. Solid-State Circuits **45**, 759 (2010).
[22]X. Wang, X. Meng, Y. Zhu, H. Ling, Y. Chen, Z. Li, M. C. Hartel, M. R. Dokmeci, S. Zhang, and A. Khademhosseini, IEEE Electron Device Lett. **42**, 46 (2021).
[23]Q. Zhang, Y. Sun, W. Xu, and D. Zhu, Adv. Mater. **26**, 6829 (2014).
[24]M. Dargusch, W. di Liu, and Z. G. Chen, Adv. Sci. **7**, 2001362 (2020).
[25]L. M. Cowen, J. Atoyo, M. J. Carnie, D. Baran, and B. C. Schroeder, ECS J. Solid State Sci. Technol. **6**, N3080 (2017).
[26]Y. Chen, Y. Zhao, and Z. Liang, Energy Environ. Sci. **8**, 401 (2015).
[27]C. Zheng, L. Xiang, W. Jin, H. Shen, W. Zhao, F. Zhang, C. Di, D. Zhu, C. Z. Zheng, L. Y. Xiang, W. L. Jin, H. G. Shen, W. R. Zhao, C. Di, D. B. Zhu, and F. J. Zhang, Adv. Mater. Technol. **4**, 1900247 (2019).
[28]J. J. Lee, D. Yoo, C. Park, H. H. Choi, and J. H. Kim, Sol. Energy **134**, 479 (2016).
[29]K. Pudzs, A. Vembris, M. Rutkis, S. K. Woodward Pudzs, A. Vembris, M. Rutkis, and S. Woodward, Adv. Electron. Mater. **3**, 1600429 (2017).
[30]M. Massetti, S. Bonfadini, D. Nava, M. Butti, L. Criante, G. Lanzani, L. Qiu, J. C. Hummelen, J. Liu, L. J. A. Koster, and M. Caironi, Nano Energy **75**, 104983 (2020).
[31]A. J. Heeger, Chem. Soc. Rev. **39**, 2354 (2010).
[32]G. Slack, *CRC Handbook of Thermoelectrics* (CRC Press, 1995).
[33]M Beekman, D. T Morelli, and G. S Nolas, Nat. Mater. **14**(12), 1182 (2015).
[34]H. Yan, N. Sada, and N. Toshima, J. Therm. Anal. Calorim. **69**(3), 881 (2002).
[35]O. Bubnova, Z. U. Khan, A. Malti, S. Braun, M. Fahlman, M. Berggren, and X.Crispin, Nat. Mater. **10**(6), 429 (2011).
[36]H. Shirakawa, E. J. Louis, A. G. MacDiarmid, C. K. Chiang, and A. J. Heeger, J. Chem. Soc., Chem. Commun. **16**, 578 (1977).
[37]R. McNeill, R. Siudak, J. H. Wardlaw, and D. E Weiss, Aust. J. Chem. **16**, 1056 (1963).
[38]A. Moliton and R. C. Hiorns, Polym. Int. **53**, 1397 (2004).
[39]A. N. Aleshin, S. R. Williams, and A. J. Heeger, Synth. Met. **94**, 173 (1998).
[40]L. Groenendaal, F. Jonas, D. Freitag, H. Pielartzik, and J. R. Reynolds, Adv. Mater. **12**, 481 (2000).
[41]L. Bießmann, N. Saxena, N. Hohn, M. A. Hossain, J. G. C. Veinot, and P. Müller-Buschbaum, Adv. Electron. Mater. **5**, 1800654 (2019).
[42]H. Shi, C. Liu, Q. Jiang, and J. Xu, Adv. Electron. Mater. **1**, 1500017 (2015).
[43]M. Cassinelli, W. T. Park, Y. Kim, J. H. Kim, Y. Y. Noh, and M. Caironi, Appl. Phys. Lett. **119**, 033301 (2021).
[44]T. A. Yemata, Y. Zheng, A. K. K. Kyaw, X. Wang, J. Song, W. S. Chin, and J. Xu, RSC Adv. **10**, 1786 (2020).
[45]M. T. Zar Myint, M. Hada, H. Inoue, T. Marui, T. Nishikawa, Y. Nishina, S. Ichimura, M. Umeno, A. K. Ko Kyaw, and Y. Hayashi, RSC Adv. **8**, 36563 (2018).
[46]Z. Fan, J. Ouyang, Z. Fan, and J. Ouyang, Adv. Electron. Mater. **5**, 1800769 (2019).
[47]L. Wang and K. Zhang, Energy Environ. Mater. **3**, 67 (2020).
[48]S. Masoumi, S. O'Shaughnessy, and A. Pakdel, Nano Energy **92**, 106774 (2022).
[49]Y. H. Lee, J. Oh, S. S. Lee, H. Kim, and J. G. Son, ACS Macro Lett. **6**, 386 (2017).
[50]I. Petsagkourakis, E. Pavlopoulou, G. Portale, B. A. Kuropatwa, S. Dilhaire, G. Fleury, and G. Hadziioannou, Sci. Rep. **6**, 30501 (2016).
[51]V. Vijayakumar, P. Durand, H. Zeng, V. Untilova, L. Herrmann, P. Algayer, N. Leclerc, and M. Brinkmann, J. Mater. Chem. C **8**, 16470 (2020).
[52]Q. Zhang, Y. Sun, F. Jiao, J. Zhang, W. Xu, and D. Zhu, Synth. Met. **162**, 788 (2012).
[53]S. Qu, Q. Yao, L. Wang, Z. Chen, K. Xu, H. Zeng, W. Shi, T. Zhang, C. Uher, and L. Chen, NPG Asia Mater. **8**, e292 (2016).
[54]H. Tang, Y. Liang, C. Liu, Z. Hu, Y. Deng, H. Guo, Z. Yu, A. Song, H. Zhao, D. Zhao, Y. Zhang, X Guo, J. Pei, Y. Ma, Y. Cao, and F. Huang, Nature **611**, 271 (2022).
[55]J. T. E. Quinn, J. Zhu, X. Li, J. Wang, and Y. Li, J. Mater. Chem. C **5**, 8654 (2017).
[56]H. Yan, Z. Chen, Y. Zheng, C. Newman, J. R. Quinn, F. Dötz, M. Kastler, and A. Facchetti, Nature **457**, 679 (2009).
[57]D. M. De Leeuw, M. M. J. Simenon, A. R. Brown, and R. E. F. Einerhand, Synth. Met. **87**, 53 (1997).
[58]J. Zaumseil and H. Sirringhaus, Chem. Rev. **107**, 1296 (2007).
[59]B. A. Jones, A. Facchetti, M. R. Wasielewski, and T. J. Marks, J. Am. Chem. Soc. **129**, 15259 (2007).
[60]J. E. Anthony, A. Facchetti, M. Heeney, S. R. Marder, and X. Zhan, Adv. Mater. **22**, 3876 (2010).
[61]J. Han, A. Chiu, C. Ganley, P. McGuiggan, S. M. Thon, P. Clancy, and H. E. Katz, Angew. Chem., Int. Ed. **60**, 27212 (2021).
[62]Y. Lu, J. Y. Wang, and J. Pei, Chem. Mater. **31**, 6412 (2019).
[63]W. Zhao, J. Ding, Y. Zou, C. A. Di, and D. Zhu, Chem. Soc. Rev. **49**, 7210 (2020).
[64]B. Saglio, M. Mura, M. Massetti, F. Scuratti, D. Beretta, X. Jiao, C. R. McNeill, M. Sommer, A. Famulari, G. Lanzani, M. Caironi, and C. Bertarelli, J. Mater. Chem. A **6**, 15294 (2018).
[65]M. Cassinelli, S. Cimò, T. Biskup, X. Jiao, A. Luzio, C. R. McNeill, Y. Y. Noh, Y. H. Kim, C. Bertarelli, and M. Caironi, Adv. Electron. Mater. **7**, 2100407 (2021).

[66]P. Wei, J. H. Oh, G. Dong, and Z. Bao, J. Am. Chem. Soc. **132**, 8852 (2010).
[67]F. Pallini, S. Mattiello, M. Cassinelli, P. Rossi, S. Mecca, W. L. Tan, M. Sassi, G. Lanzani, C. R. McNeill, M. Caironi, and L. Beverina, ACS Appl. Energy Mater. **5**, 2421 (2022).
[68]C. Y. Yang, Y. F. Ding, D. Huang, J. Wang, Z. F. Yao, C. X. Huang, Y. Lu, H. I. Un, F. D. Zhuang, J. H. Dou, C. A. Di, D. Zhu, J. Y. Wang, T. Lei, and J. Pei, Nat. Commun. **11**(1), 3292 (2020).
[69]Y. Nonoguchi, K. Ohashi, R. Kanazawa, K. Ashiba, K. Hata, T. Nakagawa, C. Adachi, T. Tanase, and T. Kawai, Sci. Rep. **3**, 719–723 (2013).
[70]Y. F. Ding, C. Y. Yang, C. X. Huang, Y. Lu, Z. F. Yao, C. K. Pan, J. Y. Wang, and J. Pei, Angew. Chem., Int. Ed. **60**, 5816 (2021).
[71]D. Schmidt, D. Bialas, and F. Würthner, Angew. Chem., Int. Ed. **54**, 3611 (2015).
[72]Y. Wang, Z. Lu, Q. Hu, X. Qi, Q. Li, Z. Wu, H. L. Zhang, C. Yu, and H. Wang, J. Mater. Chem. A **9**, 3341 (2021).
[73]H. I. Un, S. A. Gregory, S. K. Mohapatra, M. Xiong, E. Longhi, Y. Lu, S. Rigin, S. Jhulki, C.. Y. Yang, T. V. Timofeeva, J. Y. Wang, S. K. Yee, S. Barlow, S. R. Marder, and J. Pei, Adv. Energy Mater. **9**, 1900817 (2019).
[74]H. L. Smith, J. T. Dull, E. Longhi, S. Barlow, B. P. Rand, S. R. Marder, and A. Kahn, Adv. Funct. Mater. **30**, 2000328 (2020).
[75]Y. Yamashita, S. Jhulki, D. Bhardwaj, E. Longhi, S. Kumagai, S. Watanabe, S. Barlow, S. R. Marder, and J. Takeya, J. Mater. Chem. C **9**, 4105 (2021).
[76]H. Wei, P. A. Chen, J. Guo, Y. Liu, X. Qiu, H. Chen, Z. Zeng, T. Q. Nguyen, and Y. Hu, Adv. Funct. Mater. **31**, 2102768 (2021).
[77]S. Horike, Q. Wei, K. Akaike, K. Kirihara, M. Mukaida, Y. Koshiba, and K. Ishida, Nat. Commun. **13**(1), 3517 (2022).
[78]Y. Lu, J. Y. Wang, and J. Pei, Acc Chem. Res. **54**, 2871 (2021).
[79]S. Riera-Galindo, A. Orbelli Biroli, A. Forni, Y. Puttisong, F. Tessore, M. Pizzotti, E. Pavlopoulou, E. Solano, S. Wang, G. Wang, T. P. Ruoko, W. M. Chen, M. Kemerink, M. Berggren, G. di Carlo, and S. Fabiano, ACS Appl. Mater. Interfaces **11**, 37981 (2019).
[80]Y. H. Shin, H. Komber, D. Caiola, M. Cassinelli, H. Sun, D. Stegerer, M. Schreiter, K. Horatz, F. Lissel, X. Jiao, C. R. McNeill, S. Cimò, C. Bertarelli, S. Fabiano, M. Caironi, and M. Sommer, Macromolecules **53**, 5158 (2020).
[81]L. Qiu, J. Liu, R. Alessandri, X. Qiu, M. Koopmans, R. W. A. Havenith, S. J. Marrink, R. C. Chiechi, L. J. Anton Koster, and J. C. Hummelen, J. Mater. Chem. A **5**, 21234 (2017).
[82]O. Bardagot, C. Aumaître, A. Monmagnon, J. Pécaut, P. A. Bayle, and R. Demadrille, Appl. Phys. Lett. **118**, 203904 (2021).
[83]M. Xiong, X. Yan, J. Li, S. Zhang, Z. Cao, N. Prine, Y. Lu, J. Wang, X. Gu, and T. Lei, Angew. Chem. **133**, 8270 (2021).
[84]H. Guo, C.-Y. Yang, X. Zhang, A. Motta, K. Feng, Y. Xia, Y. Shi, Z. Wu, K. Yang, J. Chen, Q. Liao, Y. Tang, H. Sun, H. Y. Woo, S. Fabiano, A. Facchetti, and X. Guo, Nature **599**, 67 (2021).
[85]X. Guo and M. D. Watson, Org Lett. **10**, 5333 (2008).
[86]R. Matsidik, M. Giorgio, A. Luzio, M. Caironi, H. Komber, and M. Sommer, Eur. J. Org. Chem. **2018**, 6121–6126.
[87]A. Luzio, D. Fazzi, D. Natali, E. Giussani, K. J. Baeg, Z. Chen, Y. Y. Noh, A. Facchetti, and M. Caironi, Adv. Funct. Mater. **24**, 1151 (2014).
[88]X Guo, F. S. Kim, M. J. Seger, S. A. Jenekhe, and M. D. Watson, Chem. Mater. **24**, 1434 (2012).
[89]Z. Chen, Y. Zheng, H. Yan, and A. Facchetti, J. Am. Chem. Soc. **131**, 8 (2009).
[90]R. Matsidik, A. Luzio, S. Hameury, H. Komber, C. R. McNeill, M. Caironi, and M. Sommer, J. Mater. Chem. C **4**, 10371 (2016).
[91]S. B. Schmidt, M. Hönig, Y. Shin, M. Cassinelli, A. Perinot, M. Caironi, X. Jiao, C. R. McNeill, D. Fazzi, T. Biskup, and M. Sommer, ACS Appl. Polym. Mater. **2**, 1954 (2020).
[92]R. A. Schlitz, F. G. Brunetti, A. M. Glaudell, P. Levi Miller, M. A. Brady, C. J. Takacs, C. J. Hawker, M. L. Chabinyc, R. A. Schlitz, F. G. Brunetti, C. J. Hawker, M. L. Chabinyc, A. M. Glaudell, P. L. Miller, M. A. Brady, and C. J. Takacs, Adv. Mater. **26**, 2825 (2014).
[93]S. Wang, H. Sun, U. Ail, M. Vagin, P. O. Å. Persson, J. W. Andreasen, W. Thiel, M. Berggren, X. Crispin, D. Fazzi, and S. Fabiano, Adv. Mater. **28**, 10764 (2016).
[94]S. Fabiano, S. Braun, X. Liu, E. Weverberghs, P. Gerbaux, M. Fahlman, M. Berggren, X. Crispin, S. Fabiano, M. Berggren, X. Crispin, S. Braun, X. Liu, M. Fahlman, E. Weverberghs, and P. Gerbaux, Adv. Mater. **26**, 6000 (2014).
[95]S. Guha, F. S. Goodson, L. J. Corson, and S. Saha, J. Am. Chem. Soc. **134**, 13679 (2012).
[96]T. L. Dexter Tam, T. T. Lin, M. I. Omer, X. Wang, and J. Xu, J. Mater. Chem. A **8**, 18916 (2020).
[97]S. Guo, S. B. Kim, S. K. Mohapatra, Y. Qi, T. Sajoto, A. Kahn, S. R. Marder, and S. Barlow, Adv. Mater. **24**, 699 (2012).
[98]X. Zheng, Y. Zhang, N. Cao, X. Li, S. Zhang, R. Du, H. Wang, Z. Ye, Y. Wang, F. Cao, H. Li, X Hong, A. C. H. Sue, C. Yang, W. G. Liu, and H. Li, Nat. Commun. **9**, 1961 (2018).
[99]Y. Qi, S. K. Mohapatra, S. Bok Kim, S. Barlow, S. R. Marder, and A. Kahn, Appl. Phys. Lett. **100**, 083305 (2012).
[100]D. Kiefer, A. Giovannitti, H. Sun, T. Biskup, A. Hofmann, M. Koopmans, C. Cendra, S. Weber, L. J. Anton Koster, E. Olsson, J. Rivnay, S. Fabiano, I. McCulloch, and C. Müller, ACS Energy Lett. **3**, 278 (2018).
[101]J. Liu, L. Qiu, R. Alessandri, X. Qiu, G. Portale, J. Dong, W. Talsma, G. Ye, A. A. Sengrian, P. C. T. Souza, M. A. Loi, R. C. Chiechi, S. J. Marrink, J. C. Hummelen, L. J. A. Koster, J. Liu, L. Qiu, R. Alessandri, X. Qiu, G. Portale, J. Dong, W. Talsma, G. Ye, A. A. Sengrian, M. A. Loi, R. C. Chiechi, S. J. Marrink, J. C. Hummelen, L. J. A. Koster, and P. C. T. Souza, Adv. Mater. **30**, 1704630 (2018).
[102]F. Zhang, Y. Hu, T. Schuettfort, C. A. Di, X. Gao, C. R. McNeill, L. Thomsen, S. C. B. Mannsfeld, W. Yuan, H. Sirringhaus, and D. Zhu, J. Am. Chem. Soc. **135**, 2338 (2013).
[103]D. Adamczak, B. Passarella, H. Komber, D. Becker-Koch, O. Dolynchuk, S. B. Schmidt, Y. Vaynzof, M. Caironi, and M. Sommer, Mater. Adv. **2**, 7881 (2021).
[104]D. Nava, Y. Shin, M. Massetti, X. Jiao, T. Biskup, M. S. Jagadeesh, A. Calloni, L. Duo, G. Lanzani, C. R. Mcneill, M. Sommer, and M. Caironi, ACS Appl. Energy Mater. **1**, 4626 (2018).
[105]Y. Shin, M. Massetti, H. Komber, T. Biskup, D. Nava, G. Lanzani, M. Caironi, and M. Sommer, Adv. Electron. Mater. **4**, 1700581 (2018).
[106]Y. Lu, Z. D. Yu, H. I. Un, Z. F. Yao, H. Y. You, W. Jin, L. Li, Z. Y. Wang, B. W. Dong, S. Barlow, E. Longhi, C. Di, D. Zhu, J. Y. Wang, C. Silva, S. R. Marder, and J. Pei, Adv. Mater. **33**, 2005946 (2021).
[107]K. Shi, F. Zhang, C. A. Di, T. W. Yan, Y. Zou, X. Zhou, D. Zhu, J. Y. Wang, and J. Pei, J. Am. Chem. Soc. **137**, 6979 (2015).
[108]W. Ma, K. Shi, Y. Wu, Z. Y. Lu, H. Y. Liu, J. Y. Wang, and J. Pei, ACS Appl. Mater. Interfaces **8**, 24737 (2016).
[109]X. Y. Wang, Y. Liu, Z. Y. Wang, Y. Lu, Z. F. Yao, Y. F. Ding, Z. D. Yu, J. Y. Wang, and J. Pei, J. Polym. Sci. **60**, 538 (2022).
[110]K. Shi, Z. Y. Lu, Z. D. Yu, H. Y. Liu, Y. Zou, C. Y. Yang, Y. Z. Dai, Y. Lu, J. Y. Wang, and J. Pei, Adv. Electron. Mater. **3**, 1700164 (2017).
[111]A. Tripathi, Y. Lee, S. Lee, and H. Y. Woo, J. Mater. Chem. C **10**, 6114 (2022).
[112]C. Y. Yang, M. A. Stoeckel, T. P. Ruoko, H. Y. Wu, X Liu, N. B. Kolhe, Z. Wu, Y. Puttisong, C. Musumeci, M. Massetti, H. Sun, K. Xu, D. Tu, W. M. Chen, H. Y. Woo, M. Fahlman, S. A. Jenekhe, M. Berggren, and S. Fabiano, Nat. Commun. **12**, 2354 (2021).
[113]G. Paternò, A. J. Warren, J. Spencer, G. Evans, V. G. Sakai, J. Blumberger, and F. Cacialli, J. Mater. Chem. C **1**, 5619 (2013).
[114]J. A. Carr and S. Chaudhary, Energy Environ. Sci. **6**, 3414 (2013).
[115]J. Liu, B. van der Zee, R. Alessandri, S. Sami, J. Dong, M. I. Nugraha, A. J. Barker, S. Rousseva, L. Qiu, X. Qiu, N. Klasen, R. C. Chiechi, D. Baran, M. Caironi, T. D. Anthopoulos, G. Portale, R. W. A. Havenith, S. J. Marrink, J. C. Hummelen, and L. J. A. Koster, Nat. Commun. **11**(1), 5694 (2020).
[116]J. Liu, L. Qiu, G. Portale, M. Koopmans, G. ten Brink, J. C. Hummelen, and L. J. A. Koster, Adv. Mater. **29**, 1701641 (2017).
[117]J. Liu, L. Qiu, G. Portale, S. Torabi, M. C. A. Stuart, X. Qiu, M. Koopmans, R. C. Chiechi, J. C. Hummelen, and L. J. A. Koster, Nano Energy **52**, 183 (2018).
[118]H. Wang and C. Yu, Joule **3**, 53 (2019).
[119]O. Bubnova, Z. U. Khan, H. Wang, S. Braun, D. R. Evans, M. Fabretto, P. Hojati-Talemi, D. Dagnelund, J. B Arlin, Y. H. Geerts, S. Desbief, D. W. Breiby, J. W. Andreasen, R. Lazzaroni, W. M. Chen, I. Zozoulenko, M. Fahlman, P. J. Murphy, M. Berggren, and X. Crispin, Nat. Mater. **13**(2), 190–194 (2014).
[120]D. Scheunemann and M. Kemerink, Phys. Rev. B **101**, 075206 (2020).
[121]D. G. Cahill, S. K. Watson, and R. O. Pohl, Phys. Rev. B **46**, 6131 (1992).

[122]E. Selezneva, A. Vercouter, G. Schweicher, V. Lemaur, K. Broch, A. Antidormi, K. Takimiya, V. Coropceanu, J. L. Brédas, C. Melis, J. Cornil, and H. Sirringhaus, Adv. Mater. **33**, 2008708 (2021).
[123]O. Zapata-Arteaga, A. Perevedentsev, S. Marina, J. Martin, J. S. Reparaz, and M. Campoy-Quiles, ACS Energy Lett. **5**, 2972 (2020).
[124]G. Zuo, X. Liu, M. Fahlman, M. Kemerink, G. Zuo, M. Kemerink, X. Liu, and M. Fahlman, Adv. Funct. Mater. **28**, 1703280 (2018).
[125]S. D. Baranovskii, Phys. Status Solidi B **251**, 487 (2014).
[126]G. Zuo, Z. Li, E. Wang, M. Kemerink, G. Zuo, M. Kemerink, Z. Li, and E. Wang, Adv. Electron. Mater. **4**, 1700501 (2018).
[127]S. N. Patel, A. M. Glaudell, K. A. Peterson, E. M. Thomas, K. A. O'Hara, E. Lim, and M. L. Chabinyc, Sci. Adv. **3**, e1700434 (2017).
[128]L. Wang, Q. Yao, J. Xiao, K. Zeng, W. Shi, S. Qu, and L. Chen, Chem.—Asian J. **11**, 1955 (2016).
[129]V. Vijayakumar, Y. Zhong, V. Untilova, M. Bahri, L. Herrmann, L. Biniek, N. Leclerc, and M. Brinkmann, Adv. Energy Mater. **9**, 1900266 (2019).
[130]Y. Huang, D. H. Lukito Tjhe, I. E. Jacobs, X. Jiao, Q. He, M. Statz, X. Ren, X. Huang, I. McCulloch, M. Heeney, C. McNeill, and H. Sirringhaus, Appl. Phys. Lett. **119**, 111903 (2021).
[131]Y. Wang, K. Takimiya, Y. Wang, and K. Takimiya, Adv. Mater. **32**, 2002060 (2020).
[132]S. Schlisske, C. Rosenauer, T. Rödlmeier, K. Giringer, J. J. Michels, K. Kremer, U. Lemmer, S. Morsbach, K. Ch. Daoulas, and G. Hernandez-Sosa, Adv. Mater. Technol. **6**, 2000335 (2021).
[133]Y. Zhang, Y. Zhu, S. Zheng, L. Zhang, X. Shi, J. He, X. Chou, and Z. S. Wu, J. Energy Chem. **63**, 498 (2021).
[134]S. Janietz and D. Sainova, Macromol. Rapid Commun. **27**, 943 (2006).
[135]L. Nayak, S. Mohanty, S. K. Nayak, and A. Ramadoss, J. Mater. Chem. C **7**, 8771 (2019).
[136]E. Tekin, P. J. Smith, and U. S. Schubert, Soft Matter **4**, 703 (2008).
[137]P. Kopola, M. Tuomikoski, R. Suhonen, and A. Maaninen, Thin Solid Films **517**, 5757 (2009).
[138]L. C. Hirst and N. J. Ekins-Daukes, Prog. Photovoltaics**19**, 286 (2011).
[139]M. A. A. Mamun, M. M. Islam, M. Hasanuzzaman, and J. Selvaraj, Energy Built Environ. **3**, 278 (2022).
[140]D. Beretta, A. Perego, G. Lanzani, M. Caironi, D. Beretta, A. Perego, G. Lanzani, M. Caironi, D. Beretta, A. Perego, G. Lanzani, and M. Caironi, Sustainable Energy Fuels **1**, 174 (2017).
[141]D. Zhang, W. Y. S. Lim, S. S. F. Duran, X. J. Loh, and A. Suwardi, ACS Energy Lett. **7**, 720 (2022).
[142]H. Li, P. Mao, M. Davis, and Z. Yu, Compos. Commun. **23**, 100599 (2021).
[143]A. G. Rösch, A. Gall, S. Aslan, M. Hecht, L. Franke, M. M. Mallick, L. Penth, D. Bahro, D. Friderich, and U. Lemmer, npj Flexible Electron. **5**(1), 1 (2021).
[144]Y. Du, J. Chen, Q. Meng, J. Xu, J. Lu, B. Paul, P. Eklund, Y. Du, J. Chen, Q. Meng, J. Xu, J. Lu, B. Paul, and P. Eklund, Adv. Electron. Mater. **6**, 2000214 (2020).
[145]S. Kee, M. A. Haque, D. Corzo, H. N. Alshareef, and D. Baran, Adv. Funct. Mater. **29**, 1905426 (2019).
[146]H. Lv, L. Liang, Y. Zhang, L. Deng, Z. Chen, Z. Liu, H. Wang, and G. Chen, Nano Energy **88**, 106260 (2021).
[147]P. Cataldi, M. Cassinelli, J. A. Heredia-Guerrero, S. Guzman-Puyol, S. Naderizadeh, A. Athanassiou, and M. Caironi, Adv. Funct. Mater. **30**, 1907301 (2020).
[148]S. Mardi, P. Cataldi, A. Athanassiou, and A. Reale, Appl. Phys. Lett. **120**, 033102 (2022).
[149]N. A. Khoso, X. Jiao, X. Guangyu, S. Tian, and J. Wang, RSC Adv. **11**, 16675 (2021).
[150]T. Ding, K. H. Chan, Y. Zhou, X. Q. Wang, Y. Cheng, T. Li, and G. W. Ho, Nat. Commun. **11**(1), 6006 (2020).
[151]J. Yang, Y. Jia, Y. Liu, P. Liu, Y. Wang, M. Li, F. Jiang, X. Lan, and J. Xu, Compos. Commun. **27**, 100855 (2021).
[152]Y. Kim, A. Lund, H. Noh, A. I. Hofmann, M. Craighero, S. Darabi, S. Zokaei, J. I. Park, M.-H. Yoon, C. Müller, Y. Kim, H. Noh, J. I. Park, M. Yoon, A. Lund, A. I. Hofmann, M. Craighero, S. Darabi, S. Zokaei, and C. Müller, Macromol. Mater. Eng. **305**, 1900749 (2020).
[153]T. Sun, B. Zhou, Q. Zheng, L. Wang, W. Jiang, and G. J. Snyder, Nat. Commun. **11**(1), 572 (2020).
[154]R. A. Kishore and S Priya, Materials **11**, 1433 (2018).
[155]H. Spanggaard and F. C. Krebs, Sol. Energy Mater. Sol. Cells **83**, 125 (2004).
[156]C. W. Tang, Appl. Phys. Lett. **48**, 183 (1986).